IOP Conf. Series: Materials Science and Engineering **304** (2018) 012001 doi:10.1088/1757-899X/304/1/012001

Trace element analysis by EPMA in geosciences: detection limit, precision and accuracy

V G Batanova[1,2], A V Sobolev[1,2,3] and V Magnin[1]

[1] University Grenoble Alpes, ISTerre, CNRS, IRD, IFSTTAR, 38000 Grenoble, France
[2] Vernadsky Institute of Geochemistry and Analytical Chemistry, ul. Kosygin 19, 119991 Moscow, Russia
[3] Institut Universitaire de France, 1 rue Descartes, 75231 Paris cedex 05, France

E-mail: valentina.batanova@univ-grenoble-alpes.fr

Abstract. Use of the electron probe microanalyser (EPMA) for trace element analysis has increased over the last decade, mainly because of improved stability of spectrometers and the electron column when operated at high probe current; development of new large-area crystal monochromators and ultra-high count rate spectrometers; full integration of energy-dispersive / wavelength-dispersive X-ray spectrometry (EDS/WDS) signals; and the development of powerful software packages. For phases that are stable under a dense electron beam, the detection limit and precision can be decreased to the ppm level by using high acceleration voltage and beam current combined with long counting time. Data on 10 elements (Na, Al, P, Ca, Ti, Cr, Mn, Co, Ni, Zn) in olivine obtained on a JEOL JXA-8230 microprobe with tungsten filament show that the detection limit decreases proportionally to the square root of counting time and probe current. For all elements equal or heavier than phosphorus (Z = 15), the detection limit decreases with increasing accelerating voltage. The analytical precision for minor and trace elements analysed in olivine at 25 kV accelerating voltage and 900 nA beam current is 4 - 18 ppm (2 standard deviations of repeated measurements of the olivine reference sample) and is similar to the detection limit of corresponding elements. To analyse trace elements accurately requires careful estimation of background, and consideration of sample damage under the beam and secondary fluorescence from phase boundaries. The development and use of matrix reference samples with well-characterised trace elements of interest is important for monitoring and improving of the accuracy. An evaluation of the accuracy of trace element analyses in olivine has been made by comparing EPMA data for new reference samples with data obtained by different in-situ and bulk analytical methods in six different laboratories worldwide. For all elements, the measured concentrations in the olivine reference sample were found to be identical (within internal precision) to reference values, suggesting that achieved precision and accuracy are similar. The spatial resolution of EPMA in a silicate matrix, even at very extreme conditions (accelerating voltage 25 kV), does not exceed 7 - 8 µm and thus is still better than laser ablation inductively coupled plasma mass spectrometry (LA-ICP-MS) or secondary ion mass spectrometry (SIMS) of similar precision. These make the electron microprobe an indispensable method with applications in experimental petrology, geochemistry and cosmochemistry.

Content from this work may be used under the terms of the Creative Commons Attribution 3.0 licence. Any further distribution of this work must maintain attribution to the author(s) and the title of the work, journal citation and DOI.
Published under licence by IOP Publishing Ltd

1. Introduction

There is no rigorous definition of a trace element, and typically accepted definitions depend on the field of science. For example, in analytical chemistry, a trace element is one whose concentration is less than 100 parts per million (ppm) or less than 100 micrograms per gram; while in geochemistry, a trace element has a concentration less than 1000 ppm or 0.1 wt% of a rock's mass and substitutes for major elements in the rock-forming minerals. Reed [1] defines a trace element in wavelength dispersive X-ray spectrometry (WDS) microprobe analysis as an element with a concentration similar to the detection limit. However this definition is too complicated because the detection limit depends on analytical conditions, atomic number and measured X-ray line. Here we propose to consider an element with concentration below 1,000 ppm as a trace element and an element with concentration between 1,000 ppm and 1 wt% as a minor element.

Wavelength dispersive X-ray spectrometry electron probe microanalysis (EPMA) of minor and trace elements has several important advantages compared with other in-situ methods such as secondary ion mass spectrometry (SIMS), laser ablation inductively coupled plasma mass spectrometry (LA-ICP-MS) and micro particle-induced X-ray emission (μ-PIXE). These advantages are: the highest spatial resolution (from 1 to several micrometres); non-destructive analysis; well-developed matrix correction procedures and relatively low cost. A significant disadvantage is the sensitivity of EPMA, which is not enough to analyse elements with concentration below 10 ppm level with sufficient precision.

Traditionally EPMA has been considered as an ideal method for in-situ quantitative analysis of major and minor elements. Before the start the third millennium, only a few publications had considered the use of the microprobe for trace element analysis (e.g., [2-7]). However, significant progress in instrumental development during the last decade has allowed the EPMA to be successfully used for trace-element analyses (down to 10 ppm). These improvements include an improved stability of spectrometers and the electron column when operated at high probe current and the development of new crystal monochromators with larger areas, spectrometers with ultra-high count rates and powerful software packages. Moreover, full integration of energy-dispersive X-ray spectrometry (EDS) / WDS signals allows quantitative data for major, minor and trace elements to be collected simultaneously in a single spot. As a result EPMA is successfully used to measure trace elements in monazite (e.g., [8-10]), quartz [11-15], olivine [16-22], sulphides [23], basaltic glasses [17, 24, 25], garnet [7, 26, 27], gold [28], Fe- and Mn-oxides in soil [29], rutile [30], diamonds [31], etc.).

Theoretical aspect of trace-element analysis by EPMA have been considered in comprehensive reviews by Reed [1] and Jercinovic *et al.* [10]. In this study we concentrate on practical aspects of trace element analysis in the geosciences. All analyses presented here were produced on the JEOL JXA-8230 microprobe with tungsten filament, 5 WD and SDD ED spectrometers at ISTerre, University Grenoble Alpes, Grenoble, France.

2. Detection limit and counting statistics

The current challenge for the trace-element measurements is to decrease the detection limit (minimum detectable concentration) and to improve analytical precision (reproducibility) and accuracy.

Liebhafsky *et al.* [32] suggested that an element can be considered to be present if the value of peak intensity (N_P) exceeds the intensity of the background (N_B) by $3(N_B)^{0.5}$. The concentration at the limit of detection (C_{DL}) is expressed by different equations, among which the most frequently used are equations of [33-37]. Analytical equations show that the detection limit (DL) varies in reverse proportion to the square root of the peak-to-background ratio (P/B), the net counting rate on the peak position (P/t), and the counting time (t). Increasing of any of these parameters by a factor of 4 will decrease DL by a factor of 2. The most easily controlled parameter is counting time. Other well-known approaches to increase the characteristic X-ray signals (P/B and P/t) are to increase the beam current and the accelerating voltage (e.g., [1, 8-10, 13, 38]). Figure 1 shows the detection limit for Zn in the San Carlos olivine reference sample as function of beam current and peak counting time

at a beam acceleration voltage of 25 kV. The detection limit was determined with JEOL software using background statistics and the 3-sigma criterion [35-36]:

$$C_{DL} = 3 \text{ x } [(2N_b/T_bA_{samp})^{0.5}/((N_{std}/C_{std}) \text{ x } (i_{samp}/i_{std}))] \text{ x } 10{,}000 \quad (1)$$

where N_b is average intensity of background (cps/μA) measured on the sample, T_b is total counting time of background (s) for the sample, A_{samp} is the number of accumulation on the sample, N_{std} is net intensity on the standard (cps/μA), C_{std} is concentration in the standard (wt%), i_{samp} and i_{std} are the probe currents measured on the standard and sample (μA). We use the JEOL equation defining the detection limit, because it is determined for each analytical point by JEOL software. Obtained values are similar to those given by all equations, which use 3-sigma criterion and do not use matrix correction [32, 34-37]. To compare with detection limit equations that take into account the matrix correction [e.g., 33], one has to multiply the detection limit values obtained by eq. (1) by matrix correction coefficients. For most elements in olivine, such corrections do not exceed 10 % relative and are thus well within statistical error of the background intensity. The two exceptions are Al and P, which have ZAF correction coefficients of 1.9 and 1.6 respectively. Therefore, the detection limits for these elements are about twice and 1.5 times larger, respectively, than those obtained using the eq. (1). All relations between detection limits and beam current, counting time and accelerating voltage that are considering here are equal for all models.

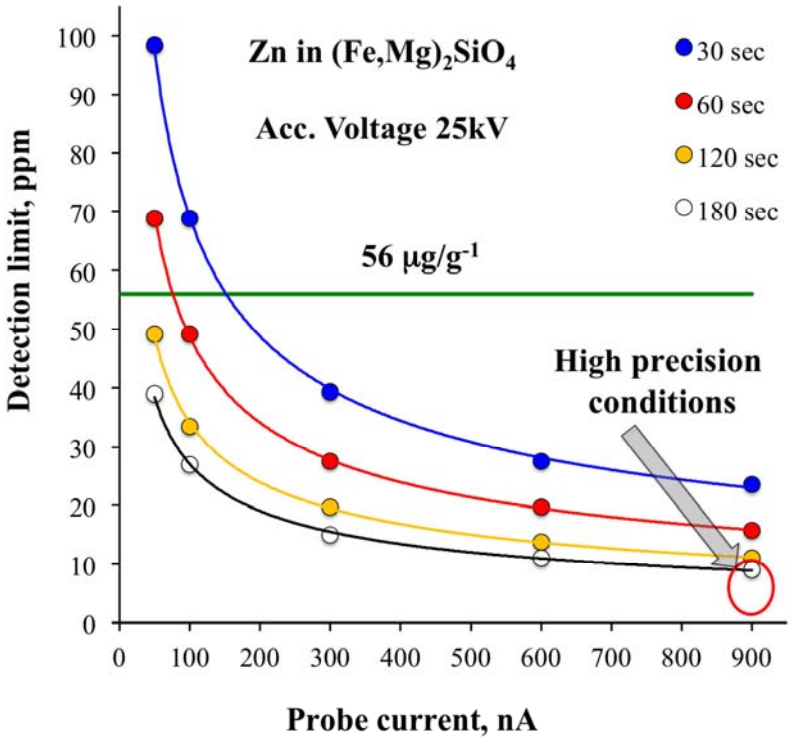

Figure 1. Detection limit for Zn in San Carlos olivine reference sample (USNM111312-44) as a function of peak counting time and beam current.

The detection limit of Zn in olivine (figure 1) behaves in accordance with counting-statistics theory: it decreases as the square root of counting time and beam current. The accepted concentration of Zn in the sample is 56 ppm (green line on figure 1, [19, 39]). Precise analysis at such low concentrations requires the combination of high probe current with long counting time (180 s and higher). Some authors have recommended to divide the long time into relatively short peak and

background measurements to minimise the effect of instrumental drift or phase instability (e.g., [1, 20, 24, 40]). The maximum precision in the determination of the background-corrected peak intensity is obtained with equal counting times for peak and background [1].

For heavy elements with atomic number (Z) > 10, the peak intensity and P/B ratio increase with increasing accelerating voltage, which therefore decreases the detection limit (e.g., [1, 10]. However, in cases of high absorption, the peak intensity passes through a maximum and then decreases. The experimental study of 10 elements (Na, Al, P, Ca, Ti, Cr, Mn, Co, Ni, Zn) in olivine shows that, for all elements starting from phosphorus (Z = 15), the detection limit decreases with increasing accelerating voltage. The behaviour of these elements is in accordance with counting statistics: DL decreases proportionally to the parameters (counting time, probe current and accelerating voltage), which leads to an increase in the peak intensity and P/B ratio (figures 2a and 2c).

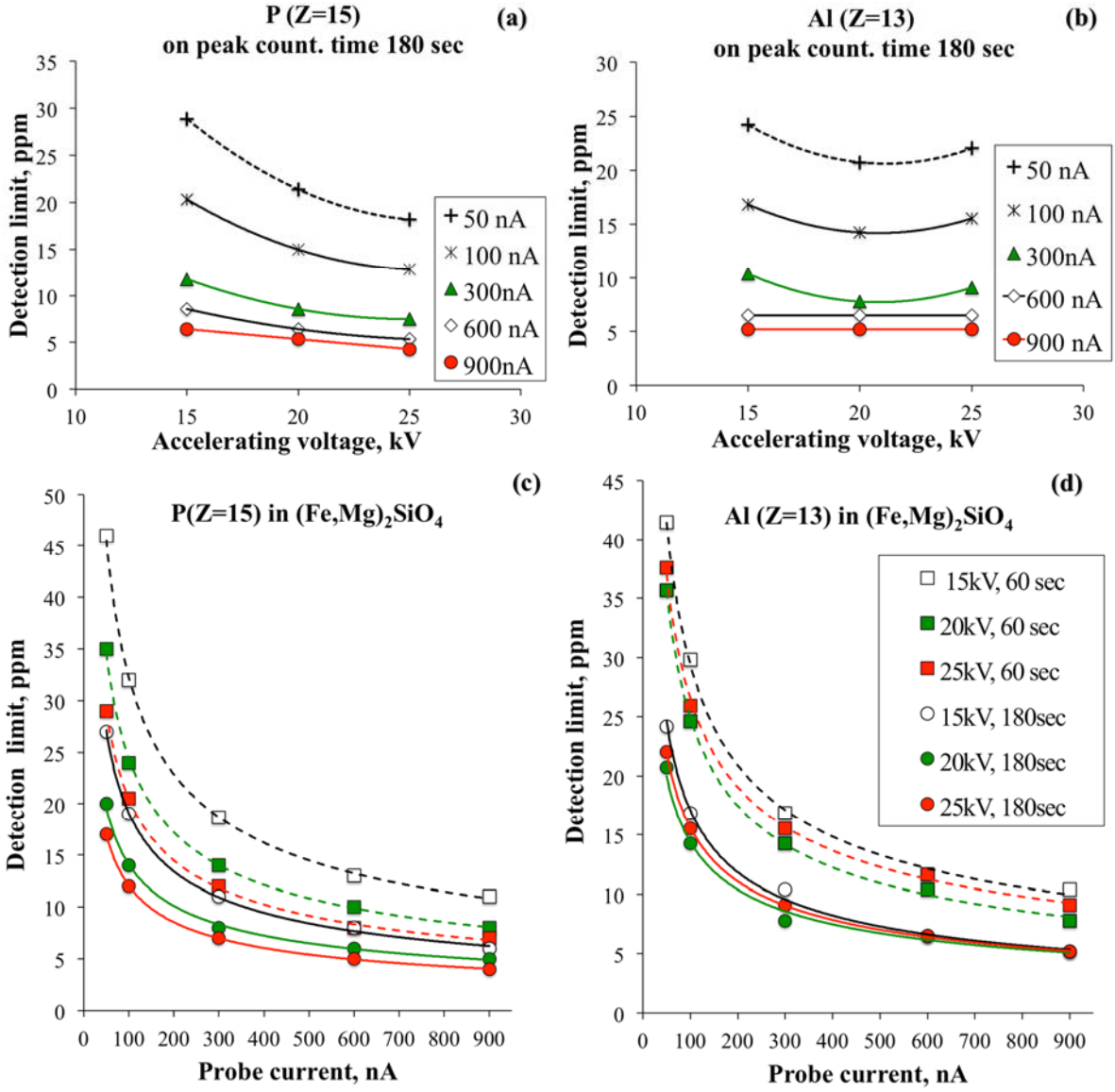

Figure 2 a-d. Detection limits for Al and P in olivine $(Fe,Mg)_2SiO_4$ matrix as a function of accelerating voltage , beam current and counting time (after [19]).

The relationship between accelerating voltage, beam current and detection limit is more complex for elements with low atomic number and, therefore, low excitation energy and high absorption coefficients (Na, Al). The detection limit at beam current up to 300 nA and long counting time (180 s on peak) decreases as accelerating voltage changes from 15 to 20 kV but then drastically increases at 25 kV (figure 2b). However, when a beam current higher than 600 nA is combined with a long counting time, the detection limit remains constant as the accelerating voltage is increased from 15 to 25 kV. This effect is not observed for short (60 s) counting times: under these conditions the detection limit increases from 20 kV to 25 kV for all probe currents (figure 2d).

Detection limits approaching the 1 ppm level can theoretically be obtained using extreme conditions (high accelerating voltage and beam current, and long counting time) [1]. Experimentally this was shown for S in steel with accelerating voltage = 20 kV and probe current = 2 µA [41].

3. Spatial resolution

It is well known that the spatial resolution decreases as accelerating voltage increases (e.g., [1, 10]). Figure 3 shows an electron flight Monte Carlo simulation of the electron interaction and X-ray generation as well as emission volumes for Al-Kα and Ni-Kα in $(Fe,Mg)_2SiO_4$ at 15, 20 and 25 kV [19]. For Ni-Kα, the X-ray generation and emission volumes have roughly equal diameters ≈ 2 µm, 4 µm and 6 µm at 15 kV, 20 kV and 25 kV, respectively. For Al-Kα, the X-ray emitted area is restricted to a depth of 2 µm for 15 kV, 20 kV, and 25 kV because of high absorption. According to Jercinovic *et al* [10] the spatial resolution of analysis (analytical resolution, AR) can be expressed as:

$$D_{AR} = (D^2_{beam} + D^2_{emission})^{0.5} \quad (2)$$

where D_{beam} is the beam diameter and $D_{emission}$ is the emission volume.

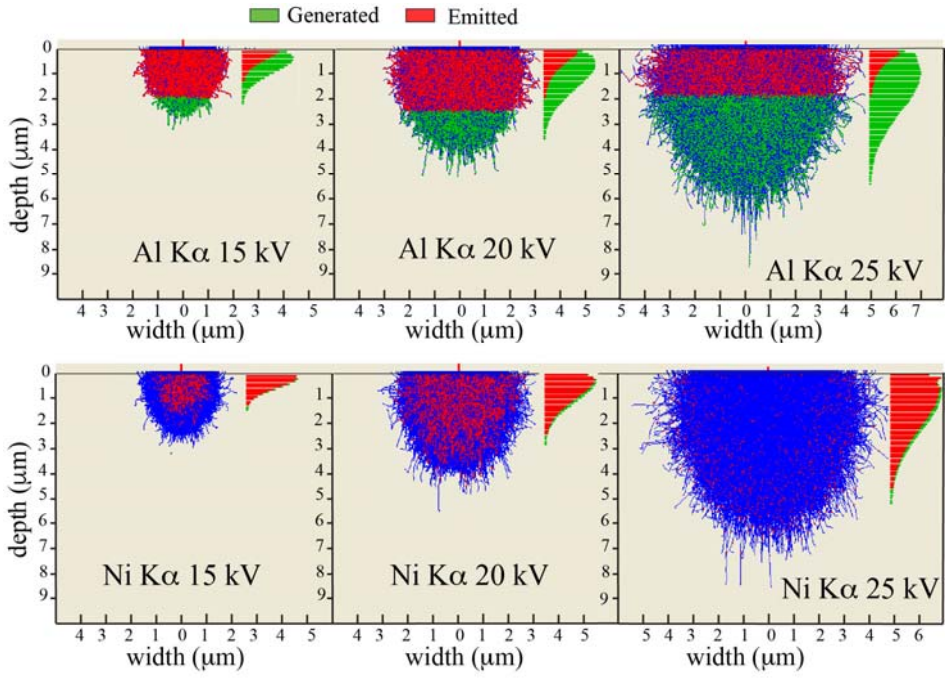

Figure 3. Monte Carlo simulation of the interaction and emission volumes of X-rays in San Carlos olivine reference sample (USNM111312-44) at 15 kV, 20 kV and 25 kV for Al-Kα and Ni-Kα. The simulation was performed using electron flight simulator (Small World, Inc.) and consists of 32,000 trials (after [19]). Printed with the permission of Chemical Geology.

Using this equation, the emission volumes listed above, and a beam diameter of 2 µm [19], we obtained a maximum diameter of the analysed area (D_{AR}) of 7.3 µm of Al-Kα for an accelerating voltage of 25 kV and a beam current of 900 nA. For accelerating voltages of 15 kV and 20 kV and a beam current of 900 nA, the diameter of the analysed area is correspondingly smaller, at 3.2 and 5.1 µm (beam diameter 1 µm [19]).

Nonetheless, the spatial resolution of EPMA of silicate minerals, even at a high accelerating voltage 25 kV, remains significantly better than with the LA-ICP-MS or SIMS. However, in the case of analysis of very small phases, the analyst has to keep accelerating voltage as low as possible (usually around 2 times of excitation energy of analysing line) and has to choose appropriate analysis times and probe currents in order to attain the required detection limit.

4. Stability, coating and optimal conditions for measurements

As discussed above, the WDS-EPMA technique requires measuring trace elements with high probe currents (hundreds of nA) and high accelerating voltages coupled with long counting times (more than few minutes) (e.g., [1, 8-10]). Thus instrumental and sample stability during long acquisition is obligatory for accurate trace element analysis. The new generation of EPMA machines provides a stable beam at high probe current for long periods. However high current beam produces significant heating of the sample surface, especially if the beam is focussed. This may damage the sample. Conductive (for both electrons and heat) materials (metals, alloys, etc.) are stable under beams with high current densities. However, the mineral phases we study in geosciences are insulators and require a conductive coating. Although various different metals (Au, Al, Ag, Cu, Be, etc.) can be used in special cases (e.g., [10] and references therein), carbon is still the most appropriate coating for EPMA. When covered with a carbon coating with thickness of about 20 - 25 nm, minerals such as olivine, orthopyroxene, some garnets, zircon, Fe and Fe-Ni sulphides remain stable under high beam currents (900 nA) during long counting time (figure 4).

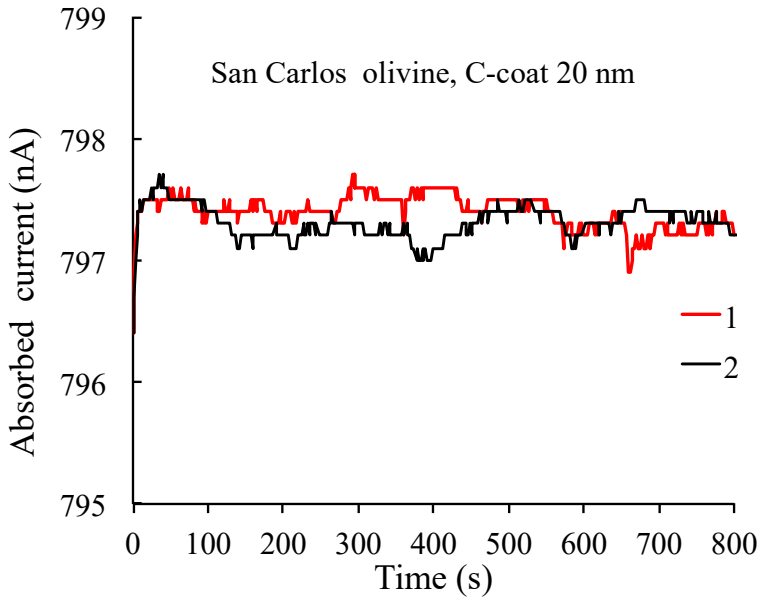

Figure 4. Absorbed current in San Carlos olivine reference sample (USNM111312-44). Beam diameter 2 µm, accelerating voltage 25 kV, beam current 900 nA, total time of beam exposure 12 min Different colour lines (1, 2) correspond to repeated measurements in different stage position within the same olivine fragment.

Figures 4 and 5 show absorbed current and signals of the trace elements during 12-minute analyses of olivine at 25 kV and 900 nA and a beam diameter of 2 µm. After 12 min of beam exposure, minor degradation of the carbon coat and slight surface damage was noted [19]. However, these effects do not have any serious impact on the stability of the absorbed current and the signal of the analysed

elements. The measured absorbed current remains constant (better than 0.05 % relative) with a 900 nA beam on olivine for an exposure time of over 720 s, the duration of a single analysis (figure 5a). The X-ray count rates of all measured trace elements show no systematic variation for exposure times exceeding 720 s (figures 5a and 5b) – 2 standard relative errors of averages are 0.1 - 0.2 % for Ni, Ti, Ca, Zn, Al, Mn, 0.3 % for Co, 0.4 % for Na and 0.7 % for P. No significant changes in X-ray counting rates occur during the first minute of analysis, even for Na (figure 5b). In addition, to estimate a possible variation and dispersion with reference to the value of the peak intensity, we normalised all intensities registered after 20 second to the mean intensity during first 20 seconds. The averages and standard deviations of these values for 700 seconds of acquisition are: Al 1.012 ± 0.031; Zn 1.001 ± 0.033; Ca 1.006 ± 0.015; Ti 1.000 ± 0.016; Ni 1.001 ± 0.014; Na 0.981 ± 0.061; Co 1.003 ± 0.042; P 0.989 ± 0.100; Mn 1.007 ± 0.024. These data indicate that deviations of normalised averages from unity are much less than their standard deviations for all measured trace elements. Also, the largest deviations from unity found for Na (2 % relative) and for Al and P (1 % relative) are equal to concentrations of 1 ppm, 2 ppm and 0.2 ppm correspondingly. We thus conclude that there are no statistically significant changes in trace element concentrations during 720 s acquisition on magnesian olivine at 900 nA beam current, 25 kV acceleration voltage and beam size of 2 µm.

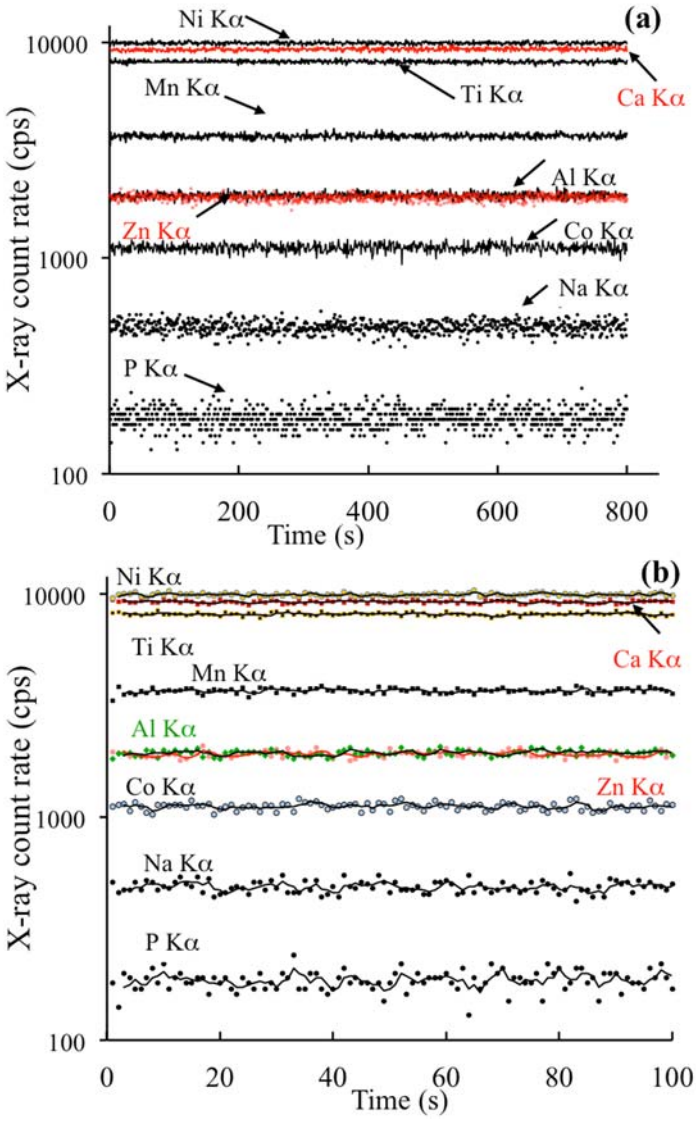

Figure 5. a) Na-Kα, P-Kα, Al-Kα, Co-Kα, Zn-Kα, Ca-Kα, Ti-Kα, Ni-Kα, and Mn-Kα line intensities as a function of time. Beam diameter 2 µm, accelerating voltage 25 kV, beam current 900 nA, total time of beam exposure 12 min (modified after [19]), and b) first 100 s of (a); lines correspond to moving 3-point averages.

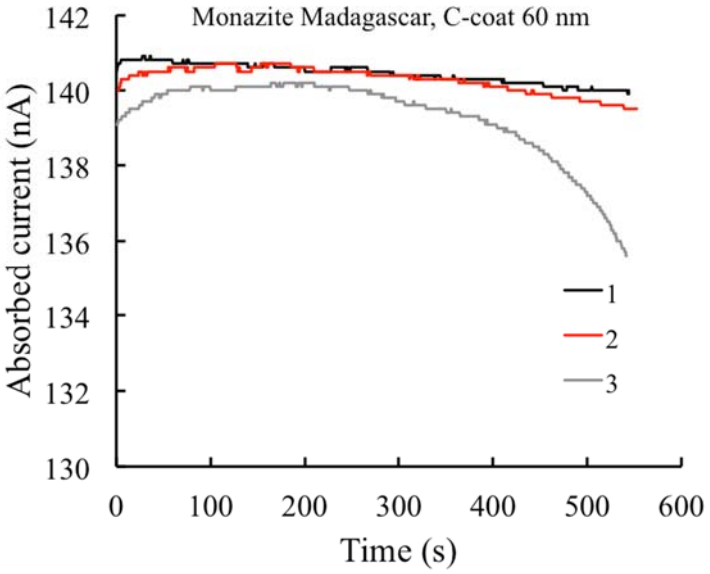

Figure 6. Absorbed current in Madagascar monazite with C-coat 60 nm as a function of time. Beam diameter 1 μm, accelerating voltage 15 kV, beam current 200 nA, total time of beam exposure 8 min. The different colour lines (1 - 3) correspond to repeated measurements in different stage position within the same monazite fragment.

We also checked the stability of major elements (measured by EDS) during typical 12-minute analyses through a series of four 3-minute analyses on the same point on San Carlos olivine. The data show no statistical differences in the measured concentrations [19] indicating that there are no significant time-dependent effects during the course of an analysis. In addition, increasing the beam diameter decreases the current density and thus improves phase stability.

Jercinovic *et al.* [8-10] considered in detail the stability of monazite with different types of coating. For the analysis of small (5 - 10 μm) monazite grains, for which the beam diameter should not exceed 1 μm, a moderate accelerating voltage (15 kV) and thick carbon coating was recommended [42]. Our experiments with the Madagascar Manangoutry monazite reference sample [43, 44] showed that the stability of this monazite improves with a carbon coating of 60 nm (figure 6). The average of normalised peak intensities (figure 7, *I*/*I*mean20, see explanation above): Dy-Lβ 1.010 ± 0.061; U-Mβ 1.006 ± 0.056, Pb-Mβ 1.009 ± 0.067 and Y-Lα 1.042 ± 0.144.

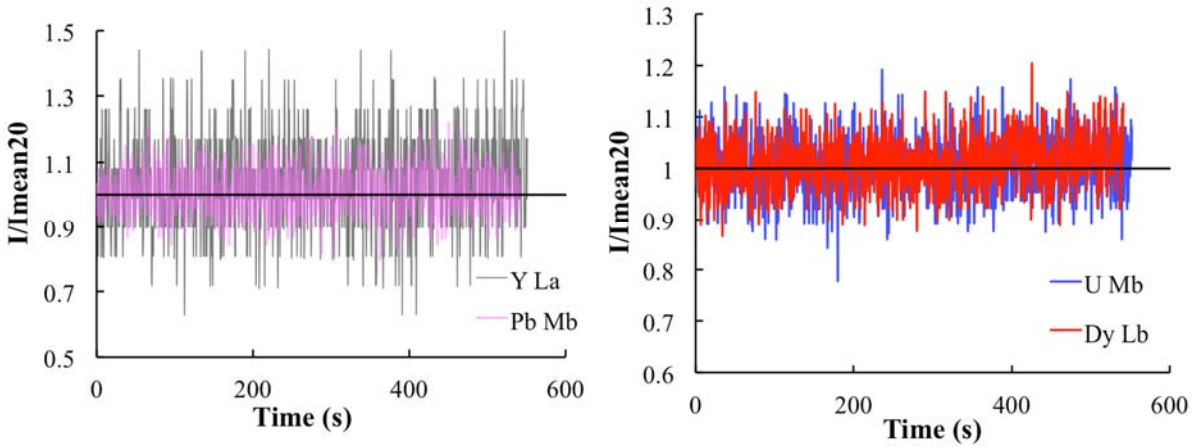

Figure 7. Normalised intensities of Dy-Lβ, U-Mβ, and Pb-Mβ, Y-Lα lines in Madagascar monazite with C-coat 60 nm as a function of time.

One should keep in mind that the standards have to be coated in the same way as samples and have a similar thickness of coating material.

Briefly, the optimal conditions for trace element analysis (accelerating voltage, beam current, counting time) should be selected taking into account: 1) the size, composition and stability of the analysing phase under the electron beam; 2) the number of trace and minor elements to be analysed and the required detection limits and precision; 3) the opportunity to use EDS for simultaneous measurement of major elements on the same point.

For phases that are unstable during long exposure under high beam current, the following measures are used in many laboratories: 1) integration (combination) of intensities using multiple spectrometers; 2) increasing the beam diameter; 3) fractional counting times at several sample positions; 4) use of a thick carbon coating or thin Au coating (e.g., [1, 8-10, 13, 42, 45]); 5) use of an iterative scheme of sample exposure in which the electron beam is cut for 10 seconds after each 10 second counting interval, allowing the sample to cool [24].

5. Accuracy and precision of trace element analysis

Given that the analytical precision in EPMA is a function of X-ray counting statistics for both peak and background, all factors that were considered above (Section 2) for the improving detection limit during trace element analysis are applicable to the precision. Mechanical reproducibility of the spectrometers is usually considered to be the limiting factor in precise measurements. Repeated measurements of trace and minor elements in olivine reference samples show that the detection limit of an element is equal to the analytical precision, calculated as 2.65 ± 0.03 standard deviations (figure 8).

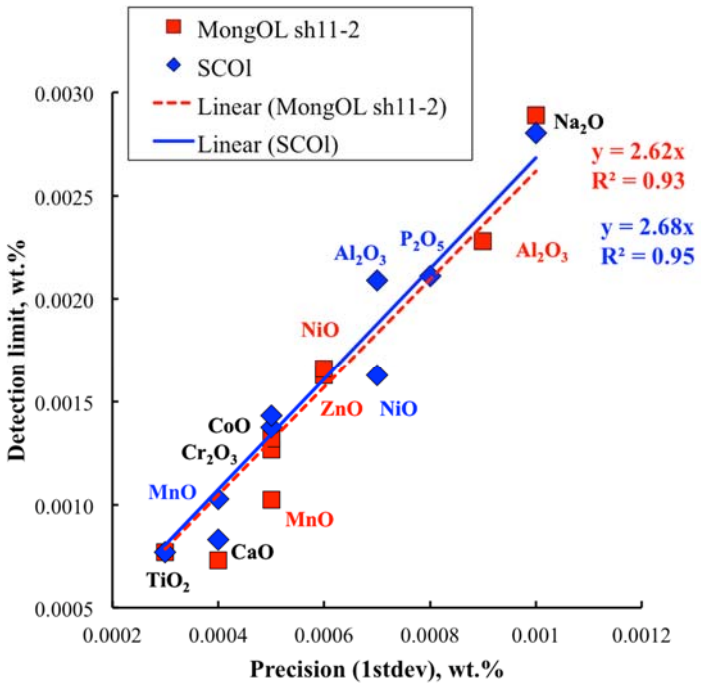

Figure 8. Relationship between detection limit (in oxides of Al, Ti, Ca, P, Na, Cr, Ni, Mn, Zn, Co) calculated by equation (1) of JEOL property software for 3 standard errors and multiplied by the ZAF correction coefficients, and reproducibility (precision) calculated as the standard deviation of 44 analyses of San Carlos olivine and 24 analyses of MongOl sh11-2 olivine reference samples measured as unknowns after each 30 - 40 analyses over a period of several days.

The accuracy of measurement by WDS for trace as well as for major elements depends on many factors including sample preparation, the type and thickness of the coating, stability under the electron beam, accurate knowledge of the composition of the primary standards, and the quality of algorithms used for matrix (i.e., the ZAF, $\varphi(\rho z)$) and interference corrections (e.g., [1, 10, 45-47]).

Jercinovic *et al.* [10] showed that the accuracy of EPMA decreases at low concentrations because most random and systematic errors encountered during major element analysis are magnified at trace level and specific errors appear. Among the special sources of errors during trace element analysis, the most important are spectral background subtraction, secondary fluorescence from phase boundaries (e.g., [48-50]), surface contamination from coating or sample preparation (e.g., [19]) and beam damage caused by high beam current and long counting times [1, 10].

5.1. Accuracy: background estimation and blank correction

One important source of systematic error during trace element analysis is poor estimation of backgrounds, because for trace elements, the peak-to-background ratio is significantly lower than for major elements [1, 10, 13, 45]. The general recommendation for accurate background estimation is a detailed WD intensity scan on the both sides of the peak of interest for the analysed sample as well as for a blank sample [1, 10, 13, 45]. The detailed WD intensity scan allows the analyst to select positions for background measurement and the appropriate method of background interpolation (classic linear, exponential or multipoint [13]. It also allows the analyst to avoid interferences on background, background discontinuities and other background artefacts such as “negative peaks” or "holes" described, for example, for LIF crystal (e.g., [1, 10, 12, 13]. Incorrect evaluation of the curvature of the continuum or different sorts of discontinuities of the continuum in the region close to the peak can bias apparent peak intensities by tens of ppm.

Figures 9 and 10 show WD intensity scans on both sides of Al-Kα on TAPJ four crystal spectrometer (Rowland circle 140 mm, P_{10} gas flow counter), and Ti-Kα for H-type (Rowland circle 100 mm) and L-type (Rowland circle 140 mm) WDS within olivine.

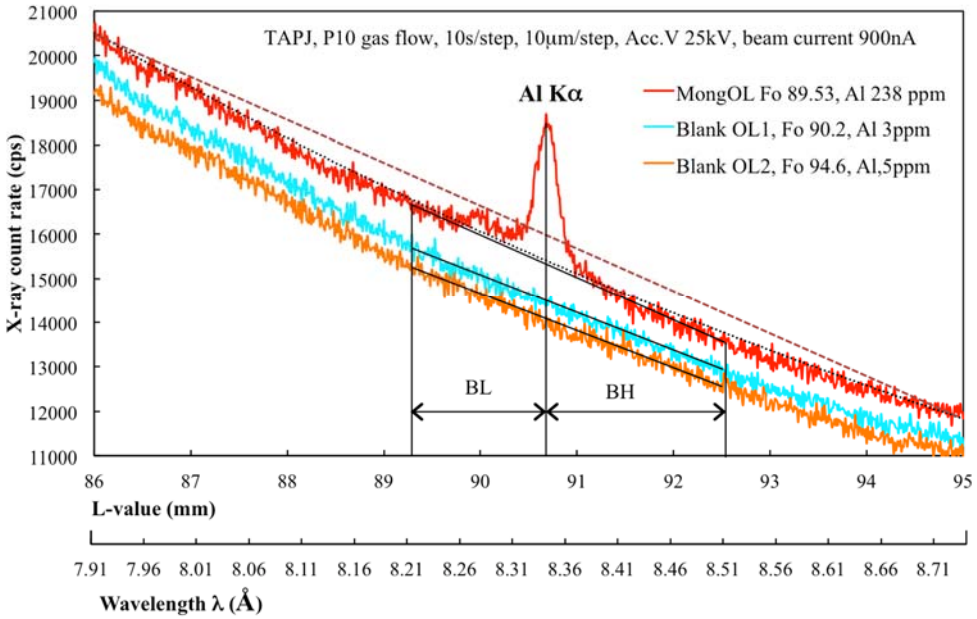

Figure 9. WD intensity scan on both sides of the Al-Kα line (TAP, P10 gas flow) in MongOl sh11-2 olivine and “blank” (Al-free) olivines with different fosterite (Fo) contents. In addition to the conditions shown on figure, counter differential mode was used (base level 0.7 V, window 9.3 V). The dashed straight line highlights the curvature of the continuum and the possibility of overestimating background intensities and underestimating Al-Kα peak intensities. The dotted line shows polynomial interpolation (e.g., [13]). BH and BL indicate the possible positions of background measurements for two points of linear interpolation model.

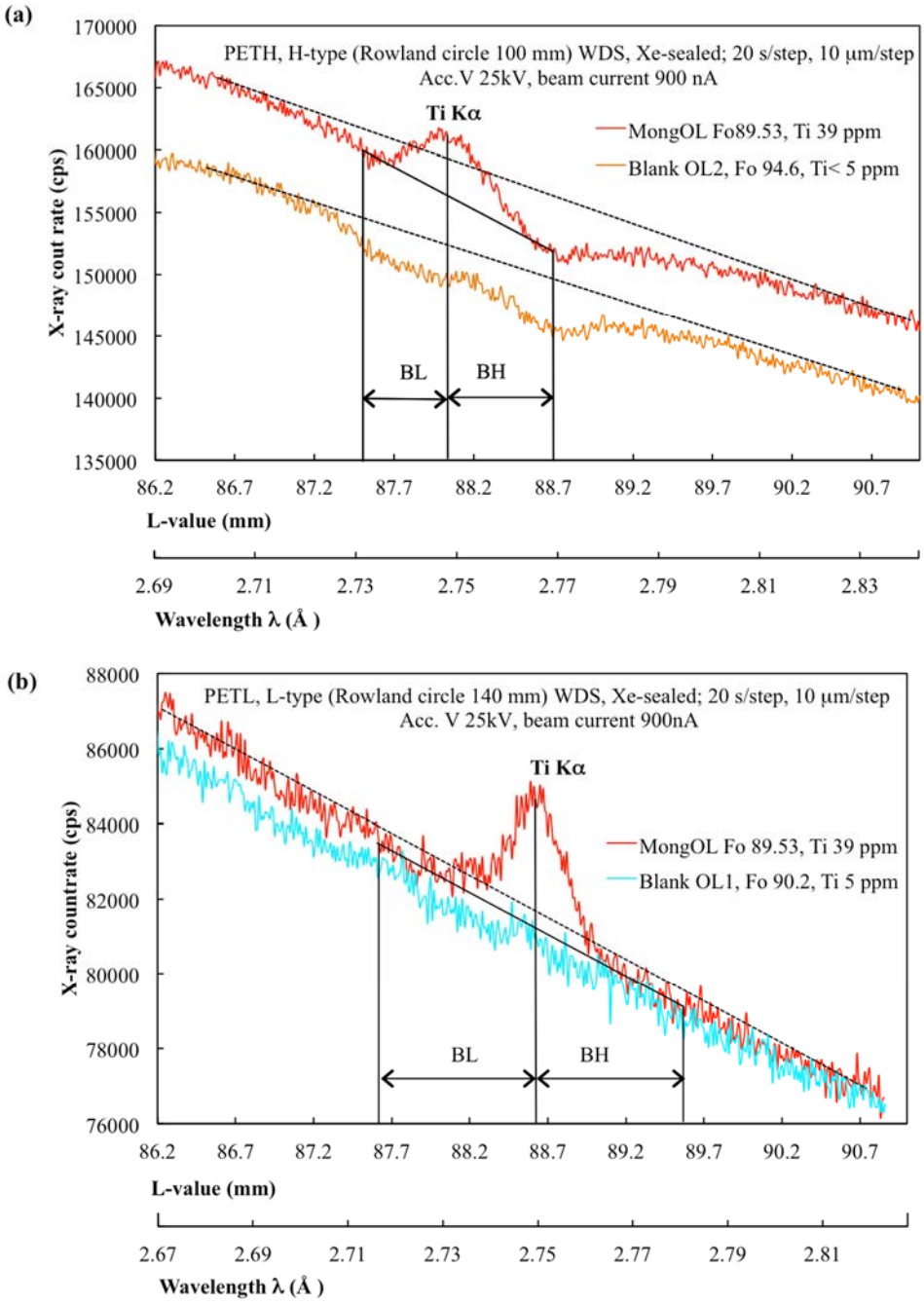

Figure 10. WD intensity scan on both sides of the Ti-Kα line for: a) H-type and b) for L-type WDS for MongOl sh11-2 olivine and "blank" olivines. In addition to the conditions shown on figures 10a and 10b, counter differential mode was used (base level 2 V, window 8 V). The dashed straight line illustrates the curvature of the continuum and the possibility of overestimating background intensities and underestimating Ti-Kα peak intensities. BH and BL indicate possible positions of background measurements for two points of linear interpolation.

The scans for Al-Kα in olivine do not reveal crystal diffraction artefacts but show the significant concave curvature of the X-ray continuum (figure 9). To avoid the negative net counts at the Al-Kα peak position, which can arise when using the classic linear background model, one should choose background positions close to the peak (BL, BH on figure 9) or select a polynomial model for background interpolation (e.g., [13]).

The position Ti-Kα is close to the spectrometer drive limit on H-type WDS. This probably results in nonlinearity of the continuum in the peak region, which is more visible on the scan of "blank" olivine (figure 10a). Use of the blank sample is important to quantify this effect (e.g., [1]). Quantitative analysis of blank olivine should produce a zero concentration when background positions are properly selected (BL, BH figure 10b). The negative concentration values obtained on the blank sample indicate problems that must be resolved before proceeding to unknowns. Minor inaccuracies from unknown sources can be corrected using a blank correction scheme. Another important task that the detailed WDS intensity scans helps to resolve is the choice of crystal. For analysis of trace concentrations of Ti (figures 10a and 10b), the L-type spectrometer is preferable because it avoids problems with linearity of continuum in the Ti-Kα region.

Classical linear interpolation of the background may be a cause of errors for complex systems such as the measurement of Pb-Mα in monazite (e.g., [1, 8-9, 13]. Possible approaches in such situations are the use of exponential or multi-point background fits, as have been developed and incorporated in Probe Software [51], as well as the use of the mean atomic number (MAN) background correction procedure based on the modelling of the continuum using Kramer's equation (e.g., [52-54]).

When the presence of a neighbouring peak rules out background measurement on one side, and only the background on the other side can be used for correction, special correction procedures are required (e.g., [1]). Sometimes an empirical solution provides very good results, as in the case of fluorine (F) analysis in Fe-bearing minerals and glasses, where the peak of F-Kα position on the sensitive LDE1 (JEOL) PC1 (CAMECA) crystals is on the "shoulder" of the Fe-$L\alpha_1$ line [24, 25].

5.2. Accuracy: analysis of reference sample

Conventional methods for trace element analysis of geological samples include running reference samples and blank samples as unknowns together with analysed samples. This allows the operator to monitor short-term systematic errors and correct for instrumental drift during long analytical sessions.

Our routine EPMA procedure includes evaluation of accuracy and precision and the monitoring of instrumental drift (e.g., [17, 19]). When analysing olivine using the Trace protocol, we usually run the olivine reference sample (San Carlos olivine USNM111312-44 [19, 39, 55]) as an unknown, three times for every 30 - 40 measurement points. We only run a blank sample as an unknown three times at the beginning and at the end of each session. All measurements of major and trace elements are corrected for deviation from San Carlos olivine reference values if the deviation is higher than 2 sigma errors. The analytical precision (reproducibility) of olivine analyses, established by repeated measurement of olivine standards, is 200 - 300 ppm (2 standard deviations) for the major element equivalent of Fo and around 4 to 18 ppm for trace elements [19]. These values are proportional to the detection limits (figure 8). We note that all three fragments of San Carlos olivine USNM111312-44 reference sample available in our laboratory are similar in composition within the errors reported above, which justifies their use as precision monitors during our Trace protocol. For concentrations of Si, Fe and Mg in the San Carlos olivine USNM111312-44 reference sample, we use data of Jarosewich *et al.* [55], while for trace and minor elements we use values from Batanova *et al.* [19]. The reliability of these values is proven by the good agreement between our data on the composition of olivine reference sample MongOl sh11-2 with data obtained by other in-situ and bulk chemical methods (see below).

More than 240 fragments of natural olivine sample (MongOl sh11-2) have been analysed using our EPMA-Trace method [19], and 120 of them were also analysed by LA-ICP-MS, SIMS and EPMA in six different laboratories world-wide [56]. The homogeneity of this olivine reference sample, within

quoted standard errors (except for Al and P), is established by EPMA and LA-ICP MS data of individual fragments. In addition, this olivine has been analysed with bulk analytical techniques (solution ICP-MS, isotope dilution and XRF). As a result of this work, preliminary reference values for major and trace elements have been estimated. Figure 11 shows comparison of data for Al and Ti obtained by our EPMA-Trace method with data obtained by other in-situ and bulk chemical methods.

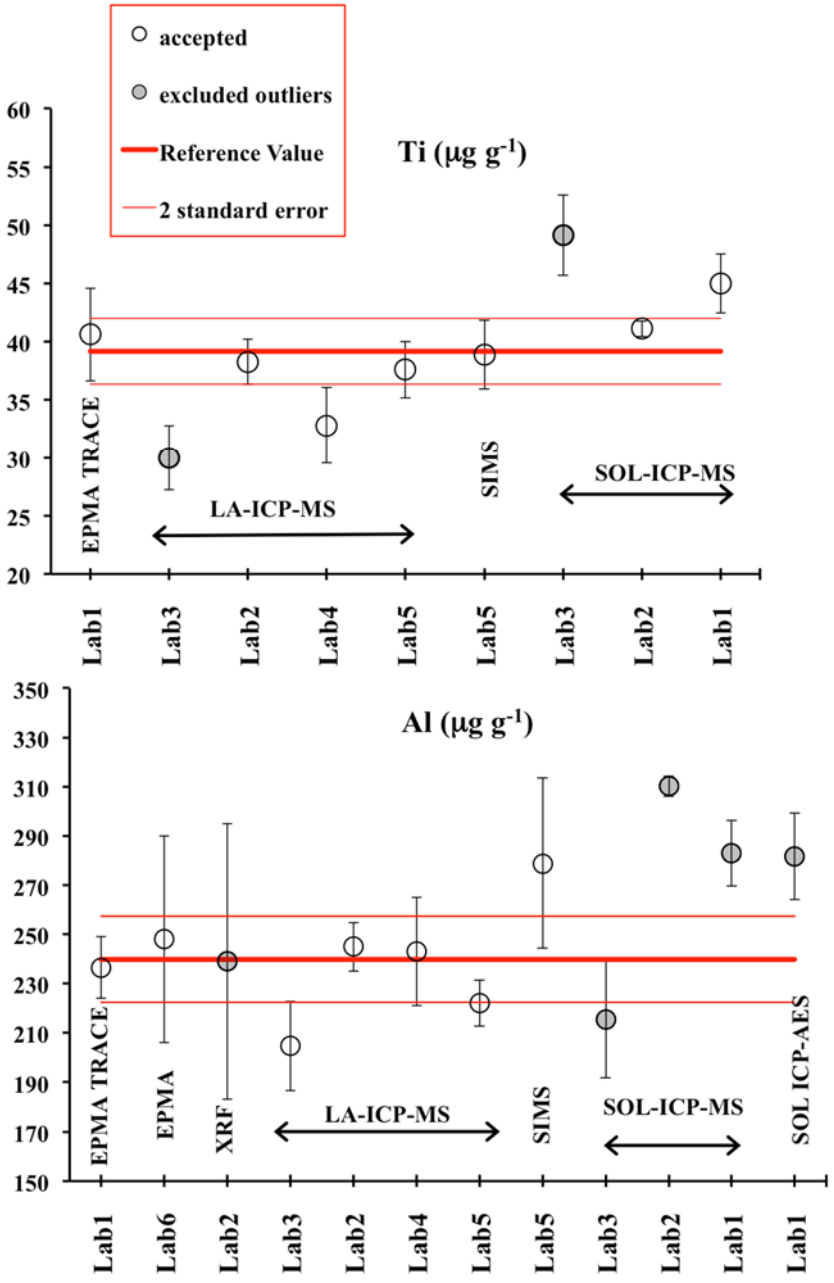

Figure 11. Trace element (Al and Ti) abundances of the new olivine reference sample MongOl sh11-2 obtained by different laboratories and analytical techniques (*in-situ* and bulk) [56]. Each value represent the mean of 120 analysis for EPMA, LA-ICP-MS and SIMS, and 1 - 3 multiply analysed aliquots for XRF, and ICP-MS. Error bars represent reported 2 standard deviations of mean.

The reference values were determined as an average of accepted values. We excluded from the averages values with 2 standard deviations outside ± 2 standard errors interval of whole population. In addition, we excluded bulk analyses for Al (figure 11) due to presence of micro inclusions of Al-rich spinel.

There is a good agreement between EPMA and other in-situ and bulk methods for 10 trace and minor elements (Na, Al, P, Ca, Ti, Cr, Mn, Co, Zn and Ni). For each element, the measured concentrations plot on the one-to-one line within the 2 standard deviations internal precision for EPMA and reference values, as shown by the error bars (figure 12). This suggests that our EPMA-Trace method for olivine is free of systematic errors and that its precision and accuracy are similar.

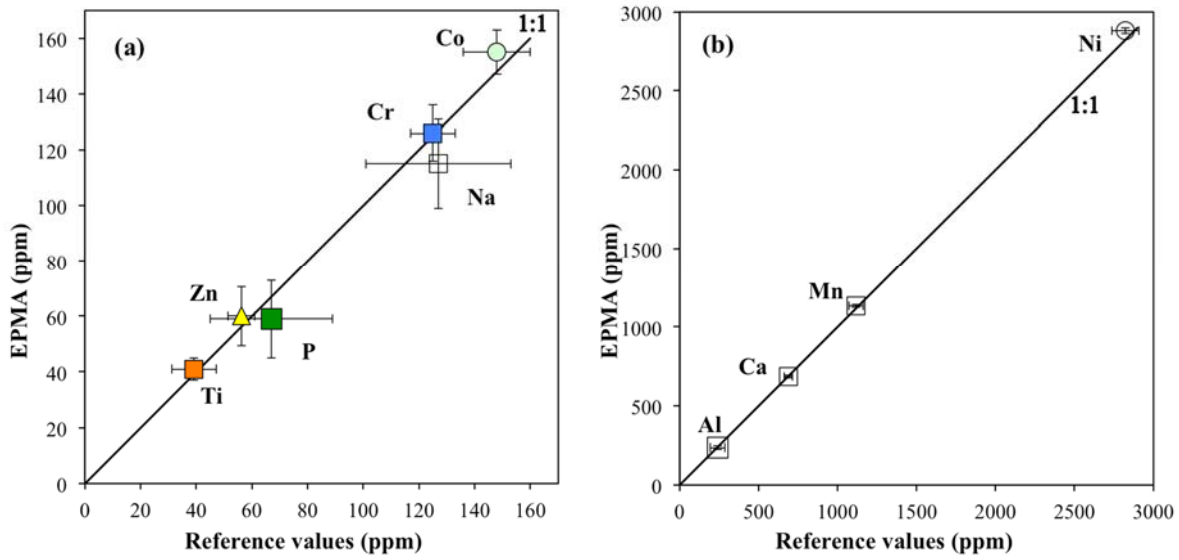

Figure 12. Comparison of trace element analyses of the new reference olivine sample MongOl sh11-2 obtained by EPMA-Trace and reference values estimated on the basis of inter laboratory *in-situ* and bulk analytical techniques [56]. Error bars for each element indicate 2 standard deviations.

6. Concluding remarks

In this study we concentrate on practical aspects of trace (below 1,000 ppm) and minor (between 1,000 ppm and 1 wt%) element analysis of geological samples. All our data and experiments were produced on the JEOL JXA-8230 microprobe with a tungsten filament, 5 WDS and SDD EDS spectrometers at ISTerre, University Grenoble Alpes, Grenoble, France. We found that:

1. The analysis of 10 elements (Na, Al, P, Ca, Ti, Cr, Mn, Co, Ni, Zn) in olivine shows that detection limits decrease proportionally to the square root of counting time and probe current. For all elements with atomic mass similar or greater than phosphorus (Z = 15), the detection limits decrease with increasing accelerating voltage. The lowest detection limit achieved in this work is 4 ppm for Ti in olivine at 25 kV acceleration voltage, 900 nA probe current and 180 s counting time for both peak and background. Repeated measurements of trace and minor elements in olivine reference samples show that the detection limit of element is equal to the analytical precision calculated as 2.65 ± 0.03 standard deviations.
2. The spatial resolution of high-precision quantitative electron microprobe analysis of silicate minerals, even at very extreme conditions (accelerating voltage = 25 kV), does not exceed 7 - 8 µm and thus is significantly better than LA-ICP-MS or SIMS of similar precision.
3. Some mineral samples with carbon-coated surfaces (thickness about 20 - 25 nm) remain stable under high beam currents (900 nA) during long counting times. Among these minerals are olivine, orthopyroxene, Fe and Fe-Ni sulphides, some garnets and zircon.

4. The accuracy of measurement by WDS for trace, minor and major elements can be evaluated by measuring reference samples with well-defined compositions similar to those of the samples. An important source of systematic error for trace elements is poorly estimated backgrounds. To obtain accurate background estimations requires a detailed WD intensity scan on the both sides of the peak of interest for both the analysed sample and a blank sample.
5. Our preferred method for trace element analysis of geological materials includes running reference samples and blank samples as unknowns together with analysed samples. This allows us to monitor short terms systematic errors and to correct for instrumental drift during long analytical sessions. Full integration of EDS/WDS signals allows us to obtain quantitative data for major, minor and trace elements simultaneously in a single spot.
6. Our routine EPMA protocol for olivine includes evaluation of accuracy and precision as well as monitoring of instrumental drift by running one or more olivine reference samples as unknowns. The analytical precision (reproducibility) of olivine analyses is 200 - 300 ppm (2 standard deviations) for the major element equivalent of Fo and between 6 and 20 ppm for trace elements. The precision is equal to the detection limits of corresponding elements. For each of 10 trace and minor elements (Na, Al, P, Ca, Ti, Cr, Mn, Co, Zn and Ni), the measured concentrations in the olivine reference was found to be same, within the 2 standard deviation internal precision, to concentrations in reference values, suggesting that our method for olivine is free of systematic errors and that accuracy is similar to precision.
7. The advantages of EPMA microanalysis of minor and trace elements over other in-situ methods such as SIMS, LA-ICP-MS and μ-PIXE are: 1) a high spatial resolution (1 - 10 μm); 2) non-destructive analysis; 3) a well-developed matrix correction procedure, and 4) relatively low cost. This makes EPMA an indispensable method with many applications in experimental petrology, geochemistry and cosmochemistry.
8. The major disadvantage of EPMA is current sensitivity, which is not sufficient to analyse elements below 10 ppm concentration levels with sufficient precision. Further advance of the EPMA technique for trace-element analysis requires the development of new ultra-high sensitive spectrometers and detectors, new background acquisition software, and development of reference materials with matrix compositions similar to analysed samples and with well-characterised trace element compositions.

Acknowledgments
VB thanks the European Microbeam Analysis Society for the invitation to the EMAS 2017 Workshop in Konstanz, Germany. We thank N. Arndt for help in improving the English and the clarity of the manuscript. The constructive critical comments of two anonymous reviewers and discussion with V.N. Korolyuk significantly improved the paper. The study was supported by a grant from Labex OSUG@2020 (Investissements d'avenir – ANR10 LABX56) and Russian Science Foundation grant 14-17-00491 to AVS.

References
[1] Reed S J B 2000 *Mikrochim. Acta* **132** 145-151
[2] Merlet C and Bodinier J L 1988 *Chem. Geol.* **70** 172-172
[3] Merlet C and Bodinier J L 1990 *Chem. Geol.* **83** 55-69
[4] Fialin M, Remy H, Richard C and Wagner C 1999 *Am. Mineral.* **84** 70-77
[5] Williams M L, Jercinovic M J and Terry M P 1999 *Geology* **27** 1023-1026
[6] Laputina I P, Batyrev V A and Yakushev A I 1999 *J. Anal. At. Spectrom.* **14** 465-469
[7] Pyle J M and Spear F S 2000 *Contrib. Mineral. Petrol.* **138** 51-58
[8] Jercinovic M J and Williams M L 2005 *Am. Mineral.* **90** 526-546
[9] Jercinovic M J, Williams M L and Lane E D 2008 *Chem. Geol.* **254** 197-215
[10] Jercinovic M J, Williams M L, Allaz J and Donovan J J 2012 *IOP Conf. Ser.:Mat. Sci. Engng.* **32** 012012

[11] Rusk B G, Reed M H, Dilles J H and Kent A J R 2006 *Am. Mineral.* **91** 1300-1312
[12] Wark D A and Watson E B 2006 *Contrib. Mineral. Petrol.* **152** 743-754
[13] Donovan J J, Lowers H A and Rusk B G 2011 *Am. Mineral.* **96** 274-282
[14] Kronz A, Kerkhof A M and Muller A 2012 *Quartz: deposits, mineralogy and analytics;* (Goetze J and Moeckel R; eds.) (Springer: Berlin, Heidelberg) 191-217
[15] Audetat A, Garbe-Schonberg D, Kronz A, Pettke T, Rusk B, Donovan J J and Lowers H A 2015 *Geostand. Geoanal. Res.* **39** 171-184
[16] Sobolev A V, Hofmann A W, Sobolev S V and Nikogosian I K 2005 *Nature* **434** 590-597
[17] Sobolev A V, Hofmann A W, Kuzmin D V, Yaxley G M, Arndt N T, Chung S L, Danyushevsky L V, Elliott T, Frey F A, Garcia M O, Gurenko A A, Kamenetsky V S, Kerr A C, Krivolutskaya N A, Matvienkov V V, Nikogosian I K, Rocholl A, Sigurdsson I A, Sushchevskaya N M and Teklay M 2007 *Science* **316** 412-417
[18] Sobolev N V, Logvinova A M, Zedgenizov D A, Pokhilenko N P, Malygina E V, Kuzmin D V and Sobolev A V 2009 *Lithos* **112** 701-713
[19] Batanova V G, Sobolev A V and Kuzmin D V 2015 *Chem. Geol.* **419** 149-157
[20] Korolyuk V N and Pokhilenko L N 2016 *Rus. Geol. Geophys.* **57** 1750-1758
[21] Sobolev A V, Asafov E V, Gurenko A A, Arndt N T, Batanova V G, Portnyagin M V, Garbe-Schonberg D and Krasheninnikov S P 2016 *Nature* **531** 628-632
[22] Zamboni D, Trela J, Gazel E, Sobolev A V, Cannatelli C, Lucchi F, Batanova V G and De Vivo B 2017 *Lithos* **272** 185-191
[23] Gervilla F, Cabri L J, Kojonen K, Oberthur T, Weiser T W, Johanson B, Sie S H, Campbell J L, Teesdale W J and Laflamme J H G 2004 *Microchim. Acta* **147** 167-173
[24] Witter J B and Kuehner S M 2004 *Am. Mineral.* **89** 57-63
[25] Zhang C, Koepke J, Wang L X, Wolff P E, Wilke S, Stechern A, Almeev R and Holtz F 2016 *Geostand. Geoanal. Res.* **40** 351-363
[26] Lavrent'ev Y G, Korolyuk V N, Usova L V and Logvinova A M 2006 *Rus. Geol. Geophys.* **47** 1075-1078
[27] Borghi A, Cossio R, Olmi F, Ruffini R and Vaggelli G 2002 *Mikrochim. Acta* **139** 17-25
[28] Gauert C, Schannor M, Hecht L, Radtke M and Reinholz U 2016 *Geostand. Geoanal. Res.* **40** 267-289
[29] Neaman A, Martinez C E, Trolard F and Bourrie G 2008 *Appl. Geochem.* **23** 778-782
[30] Spear F S, Wark D A, Cheney J T, Schumacher J C and Watson E B 2006 *Contrib. Mineral. Petrol.* **152** 375-385
[31] Weiss Y, Griffin W L, Elhlou S and Navon O 2008 *Chem. Geol.* **252** 158-168
[32] Liebhafsky H A, Pfeiffer H G and Zemany P D 1960 in: *2nd International Symposium: X-ray Microscopy and X-ray Microanalysis.* (Engstrom A, Cosslet V and Pattee H; eds.) (Elsevier, Amsterdam) 321
[33] Ancey M, Bastenaire F and Tixier R 1978 in: Proc. *Summer School St. Martin-d'Herres.* (Maurice F; ed.) (Orsay, France: Les Editions de Physique) 319-343
[34] Ziebold T O 1967 *Anal. Chem.* **39** 858-861
[35] Sato A, Mori N, Takakura M and Notoya S 2007 *JEOL News* **42** 46-52
[36] Goldstein J, Newbury D, Joy D, Lyman C, Echlin P, E. L, Sawyer L and Michael J 2003 *Scanning electron microscopy and X-ray microanalysis.* (New York, NY: Springer) 690
[37] Toya T and Kato A 1983 *Practical techniques for microprobe analysis.* (Tokyo, Japan: JEOL Training Center)
[38] Lavrent'ev Y G 2010 *X-ray Spectrom.* **39** 37-40
[39] De Hoog J C M 2008 *Geochim. Cosmochim. Acta* **72** A208-A208
[40] Korolyuk V N and Pokhilenko L N 2014 *X-ray Spectrom.* **43** 353-358
[41] Mori N, Kamiyama R, Tanaka T, Kimura T, McSwiggen P, Onodere H and Nielsen C 2013 *Microsc. Microanal.* **19** (Suppl. 2) 1432

[42] Montel J M, Razafimahatratra D, Ralison B, De Parseval P, Thibault M and Randranja R 2011 *Europ. J. Mineral.* **23** 745-757 [43] Montel J M, Foret S, Veschambre M, Nicollet C and Provost A 1996 *Chem. Geol.* **131** 37-53
[44] Seydoux-Guillaume A M, Wirth R, Deutsch A and Scharer U 2004 *Geochim. Cosmochim. Acta* **68** 2517-2527
[45] Rinaldi R and Llovet X 2015 *Microsc. Microanal.* **21** 1053-1069
[46] Lifshin E and Gauvin R 2001 *Microsc. Microanal.* **7** 168-177
[47] Gunn J S, Harrowfield I R, Proctor C H and Thresher R E 1992 *J. Exp. Mar. Biol. Ecol.* **158** 1-36
[48] Dalton J A and Lane S J 1996 *Am. Mineral.* **81** 194-201
[49] Llovet X, Galan G 2003 *Am. Mineral.* **88** 121-130
[50] Llovet X, Pinard P T, Donovan J J and Salvat F 2012 *J. Phys. D:Appl. Phys.* **45**
[51] Probe software Inc., 885 Crest Drive, Eugene, OR 97405, USA
[52] Donovan J J and Tingle T N 1996 *J. Microsc. Microanal.* **2** 1-7
[53] Laputina I P and Batyrev V A 1998 *Mikrochim. Acta* **Suppl. 15** 247-252
[54] Donovan J J, Singer J W and Armstrong J T 2016 *Am. Mineral.* **101** 1839-1853
[55] Jarosewich E J, Nelen J A and Norberg J A 1980 *Geostand. Newslett.* **4** 43-47
[56] Batanova V, Sobolev A, Thompson J M, Danyushevsky L V, Goemann K, Portnyagin M V, Garbe-Schonberg D, Hauri E H, Kimura J-I, Chang Q, Senda R, Chauvel C, Campillo S and Ionov D 2017 *Goldschmidt Conference.* (Paris, France)